Density functional theory of the Seebeck coefficient in the Coulomb blockade regime

Kaike Yang,[1] Enrico Perfetto,[2,3] Stefan Kurth,[1,4] Gianluca Stefanucci,[2,3] and Roberto D'Agosta[1,4]

[1]*Nano-Bio Spectroscopy Group and European Theoretical Spectroscopy Facility (ETSF), Departamento de Física de Materiales, Universidad del País Vasco UPV/EHU, Avenida de Tolosa 72, E-20018 San Sebastián, Spain*

[2]*Dipartimento di Fisica and European Theoretical Spectroscopy Facility (ETSF), Università di Roma Tor Vergata, Via della Ricerca Scientifica 1, 00133 Rome, Italy*

[3]*INFN, Laboratori Nazionali di Frascati, Via E. Fermi 40, 00044 Frascati, Italy*

[4]*IKERBASQUE, Basque Foundation for Science, E-48013, Bilbao, Spain*

The Seebeck coefficient plays a fundamental role in identifying the efficiency of a thermoelectric device. Its theoretical evaluation for atomistic models is routinely based on density functional theory calculations combined with the Landauer-Büttiker approach to quantum transport. This combination, however, suffers from serious drawbacks for devices in the Coulomb blockade regime. We show how to cure the theory through a simple correction in terms of the *temperature derivative* of the exchange correlation potential. Our results compare well with both rate equations and experimental findings on carbon nanotubes.

The quest for increasingly energy-efficient technologies has recently led to significant scientific and technological interest in thermoelectricity [1–4]. Indeed, thermoelectric devices convert waste heat to electric power: The basic working principle at their heart is the Seebeck effect [5]. The corresponding Seebeck coefficient is an important ingredient in the thermoelectric figure of merit (an efficiency measure of a thermoelectric device). At present, the method of choice for an atomistic modeling of the Seebeck and other transport coefficients is density functional theory (DFT) combined with the Landauer-Büttiker formalism (LB-DFT) [6,7]. However, an incautious use of LB-DFT as guide to material and system selection may point in the wrong direction. In fact, LB-DFT is unable to capture the ubiquitous Coulomb blockade (CB) phenomenon of quantum devices weakly coupled to leads, thereby overestimating the conductance and, as we shall see, underestimating the Seebeck coefficient. In Refs. [8–10] it was shown that the erroneous high conductance predicted by LB-DFT stems from neglecting exchange-correlation (xc) corrections to the bias [11–15]. According to a recently proposed DFT framework for thermal transport (and thus for the calculation of the Seebeck coefficient) [16,17] xc corrections to the temperature gradient are also expected to occur.

In this Rapid Communication we propose an alternative DFT approach to the Seebeck coefficient well suited for quantum devices in the CB regime. Following a recent idea on the construction of xc corrections to the conductance [8], we find a very simple xc correction to the LB-DFT Seebeck coefficient in terms of static DFT quantities. To illustrate the theory we first consider the Anderson impurity model (AIM), a paradigm for the CB effect [18], and subsequently extend the analysis to multiple-level systems. The proposed equations are validated by benchmarking the results against those of the rate equations [19–21] (RE), demonstrating the crucial role of the xc correction. Finally, we apply the theory to single-wall carbon nanotubes and find good qualitative agreement with experiment.

The Seebeck coefficient S is defined as the ratio $S = (\Delta V / \Delta T)_{I=0}$, where ΔV is the voltage that must be applied

to cancel the current I generated by a small temperature difference ΔT between the left and right leads. This definition corresponds to the phenomenological Seebeck coefficient of Refs. [22,23]. For an AIM symmetrically coupled to featureless leads the Seebeck coefficient takes the form [24] (atomic units are used throughout)

$$S = -\frac{1}{T} \frac{\int \omega f'(\omega) A(\omega)}{\int f'(\omega) A(\omega)}, \quad \int \equiv \int_{-\infty}^{\infty} \frac{d\omega}{2\pi}, \quad (1)$$

with $A(\omega)$ being the interacting spectral function, $f(\omega) = 1/(1 + e^{\beta(\omega-\mu)})$ being the Fermi function at temperature $T = 1/\beta$ and chemical potential μ, and $f' \equiv df/d\omega$. We now show how to rewrite S in terms of quantities which are *all* accessible by DFT. The starting point is the many-body (MB) equation $N = 2 \int f(\omega) A(\omega)$ for the electron occupation at the impurity. For an uncoupled impurity A depends on T and μ exclusively through N. This exact property is also a very good approximation at weak coupling and in the CB regime [25]. Hence the MB equation can be converted into a self-consistent equation for N, and at the self-consistent solution we can write $dA/dT = (dA/dN)(dN/dT)$. After some algebra we find

$$\frac{dN}{dT} = -\frac{2}{T} \frac{\int \omega f'(\omega) A(\omega)}{1 + R}, \quad (2)$$

where we have defined $R = -2 \int f(\omega) dA(\omega)/dN$. With similar steps we can also express the compressibility as

$$\frac{dN}{d\mu} = -\frac{2 \int f'(\omega) A(\omega)}{1 + R}. \quad (3)$$

The combination of Eqs. (2) and (3) then gives

$$S = -\frac{dN/dT}{dN/d\mu}. \quad (4)$$

This rewriting of the Seebeck coefficient is extremely interesting from a DFT perspective since it involves exclusively the occupation N of the *equilibrium* system. We then calculate the derivatives in Eq. (4) using the Kohn-Sham (KS) expression $N = 2 \int f(\omega) A_s(\omega)$, where A_s is the KS spectral function. For a gated impurity with energy v we have

$A_s(\omega) = \ell(\omega - v - v_{\text{Hxc}})$, with $\ell(\omega) = \gamma/(\omega^2 + \gamma^2/4)$ being a Lorentzian of width determined by the dot-lead tunneling rate $\gamma/2$. The Hartree-xc (Hxc) potential v_{Hxc} depends on N and T. Therefore, at self-consistency A_s depends implicitly (through N) on μ and both implicitly and explicitly on T. By calculating the required density derivatives and taking into account that $\frac{dv_{\text{Hxc}}}{dT} = (\frac{\partial v_{\text{Hxc}}}{\partial N})_T \frac{dN}{dT} + (\frac{\partial v_{\text{Hxc}}}{\partial T})_N$, we obtain the *exact* relation

$$S = S_s + \left(\frac{\partial v_{\text{Hxc}}}{\partial T}\right)_N. \tag{5}$$

Here S_s is the KS Seebeck coefficient obtained from Eq. (1) by replacing $A(\omega)$ with $A_s(\omega)$, and it is precisely the coefficient predicted by the LB-DFT approach. We further observe that for the derivation of Eq. (5) it is not necessary that A_s is a Lorentzian; the only requirement is that A_s is a function of $(\omega - v - v_{\text{Hxc}})$.

Equation (5), the central result of this Rapid Communication, provides a rigorous route to cure LB-DFT through the inclusion of the xc correction $\partial v_{\text{Hxc}}/\partial T$ while still remaining in a pure DFT framework. As we shall see, Eq. (5) also suggests how to correct S_s in larger systems.

At temperatures $T \gg \gamma$, but still $T \ll U$ where U is the onsite repulsion, the CB phenomenon leaves clear fingerprints on the Seebeck coefficient. Nevertheless, these are only partially captured by S_s, even when the exact v_{Hxc} is used (see below). The Anderson model is particularly instructive since it allows us to disentangle the coordinated actions of the CB effect on S_s and of the xc correction in reproducing the interacting S.

In the following we assume that γ is the smallest energy scale and we approximate v_{Hxc} by the exact Hxc potential of the isolated ($\gamma = 0$) impurity [26,27],

$$v_{\text{Hxc}}[N] \approx v_{\text{Hxc}}^{\text{imp}}[N] = \frac{U}{2} + g_U(N - 1), \tag{6}$$

where $g_U(x) = \frac{U}{2} + \frac{1}{\beta} \ln\left(\frac{x + \sqrt{x^2 + \exp(-\beta U)(1 - x^2)}}{1 + x}\right)$. At low temperatures, the Hxc potential exhibits a sharp (but continuous) step of size U at occupation $N = 1$ [26,28,29]. With an analytic expression for v_{Hxc} we can evaluate both terms on the right-hand side of Eq. (5). In Fig. 1 we show S calculated from our DFT equation (black) versus the gate v. To demonstrate the accuracy of the result we also show the Seebeck coefficient calculated from Eq. (1) using the MB spectral function $A(\omega) = \frac{N}{2}\ell(\omega - v - U) + (1 - \frac{N}{2})\ell(\omega - v)$ [25] (blue) as well as the one calculated using the RE approach of Ref. [20] (red), exact in the limit $\gamma \to 0$. All three approaches give the same Seebeck coefficient and densities (see inset). Let us now discuss how the two terms in Eq. (5) contribute. The KS Seebeck S_s (green) accounts for the correct linear behavior (with slope proportional to T^{-1}) at large values of $|v|$. In fact, for $\gamma \to 0$ the KS spectral function becomes $A_s(\omega) = 2\pi\delta(\omega - v - v_{\text{Hxc}})$ and consequently $S_s = -(v + v_{\text{Hxc}})/T$. The linear behavior at large $|v|$ is not surprising since the noninteracting Seebeck coefficient behaves in the same way. Noteworthy is instead the plateau of S_s for $v \in (-U, 0)$. This is a direct consequence of the step in v_{Hxc} which pins the KS level to the chemical potential, thereby blocking electrons with energy below $v + U$ from entering the impurity site
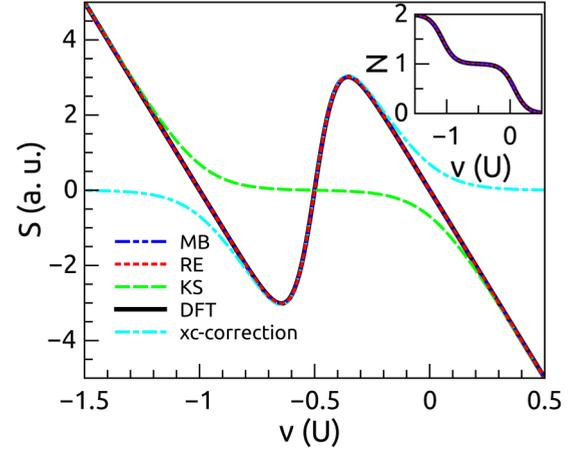

FIG. 1. Seebeck coefficient S and density N (inset) for the Anderson model vs gate v for our corrected DFT (black), MB (blue), and RE (red). The S_s (KS, green) and the xc correction $\partial v_{\text{Hxc}}/\partial T$ (cyan) are also displayed. The parameters are $T = 0.1$ and $\gamma = 0.01$ (energies in units of U).

(see inset). The CB-induced plateau in S_s opens a gap in the noninteracting straight line $-v/T$, shifting it leftward by U for $v < -U$ and generating the correct behavior at large negative values of v. However, S_s misses entirely the oscillation of S for $N \approx 1$, thus severely underestimating the true Seebeck coefficient. Remarkably, this deficiency is exactly cured by the xc correction $\partial v_{\text{Hxc}}/\partial T$ (cyan). The temperature variation of v_{Hxc} is the key ingredient for the nonvanishing Seebeck coefficient in the CB regime [20,30–32]. We emphasize that the LDA potential misses both the plateau (no step in v_{Hxc}) and the oscillation induced by $\partial v_{\text{Hxc}}/\partial T$ [33].

We now extend the DFT approach to junctions with more than one level. For $T \gg \gamma$ the Seebeck coefficient exhibits a sawtooth behavior as a function of v, with rapid (but continuous) jumps occurring when the number N of electrons crosses an integer. Furthermore, if the level spacing $\Delta\varepsilon$ is much larger than T, a superimposed fine structure of wiggles spaced by $\Delta\varepsilon$ emerges [20]. The wiggles originate from excitations that bring the system with $(N - 1)$ particles in the ground state to some excited state with N particles.

The physics of the Seebeck coefficient in a multiple-level junctions is well captured by the constant interaction model (CIM). The CIM Hamiltonian reads $\hat{H} = \sum_{i\sigma} \varepsilon_i \hat{n}_{i\sigma} + \frac{1}{2} \sum_{i\sigma \neq j\sigma'} U_{ij} \hat{n}_{i\sigma} \hat{n}_{j\sigma'}$, where $\hat{n}_{i\sigma}$ is the occupation operator of the ith level with spin σ. The indices i, j run over M levels and for $M = 1$ we are back to the Anderson model. For simplicity we assume that each level is equally coupled to the left and right leads with tunneling rate $\gamma/2$. In this case the derivation of Eq. (4) can be repeated step by step by replacing the spectral function A with its trace $\text{Tr}[A]$. Consequently, we can again express S in a pure DFT framework by calculating the derivatives of the total number of electrons from the KS expression $N = 2 \int f(\omega) \text{Tr}[A_s(\omega)]$. The KS spectral function $[A_s]_{ij} = \delta_{ij} A_{s,i}$ is diagonal in the level basis and reads $A_{s,i}(\omega) = \ell(\omega - \varepsilon_i - v_{\text{Hxc},i})$, where the Hxc potential of level i depends on the occupations $\{n\}$ of all the levels. It is

straightforward to show that

$$S = S_s + \sum_j \frac{\int f'(\omega) A_{s,j}(\omega)}{\int f'(\omega) \text{Tr}[A_s(\omega)]} \left(\frac{\partial v_{\text{Hxc},j}}{\partial T} \right)_N. \tag{7}$$

In Ref. [34] we proved that at zero temperature the Hxc potential of the isolated ($\gamma = 0$) CIM Hamiltonian is uniform and depends only on N, i.e., $v_{\text{Hxc},i}[\{n\}] = v_{\text{Hxc}}[N]$. The zeroth-order approximation at finite temperatures and weak coupling to the leads therefore consists in neglecting the nonuniformity and the local dependence on the $\{n\}$. In this approximation Eq. (7) reduces to Eq. (5). The interacting Seebeck coefficient then follows once we specify the functional form of v_{Hxc}. Following Ref. [8] we construct $v_{\text{Hxc}}[N]$ as the sum of single-impurity Hxc potentials according to

$$v_{\text{Hxc}}[N] = \sum_{K=1}^{2M-1} \left[\frac{U_K}{2} + g_{U_K}^{\text{ext}}(N - K) \right], \tag{8}$$

where U_K is the charging energy needed for adding one electron to the system with K electrons, and the extended g_U^{ext} function is defined according to

$$g_U^{\text{ext}}(N-1) = \begin{cases} -U/2 & N < 0 \\ g_U(N-1) & 0 \leqslant N \leqslant 2 \\ U/2 & N > 2 \end{cases}, \tag{9}$$

with g_U given below Eq. (6). The Hxc potential in Eq. (8) has a staircase behavior with steps of width U_K between two consecutive integers.

To assess the quality of our approximate Hxc potential we first consider a two-level CIM with $U_{ij} = U$. In Fig. 2 we display results at temperature $T = 0.03$, coupling $\gamma = 0.001$, and $\varepsilon_i = \varepsilon_i^0 + v$, where $\varepsilon_1^0 = 0$ and $\varepsilon_2^0 = 0.3$ (energies in units of U). The left panel shows the total occupation N as well as the occupation $n_2 = \sum_\sigma n_{2\sigma}$ of the highest level calculated using both DFT and RE. Although a perfect agreement is found for N, exponentially small discrepancies are seen for the local occupation. In fact, the uniformity (i.e., level independence) of our zeroth-order approximation v_{Hxc} of Eq. (8) neglects thermal excitations, which corresponds to mixing only ground
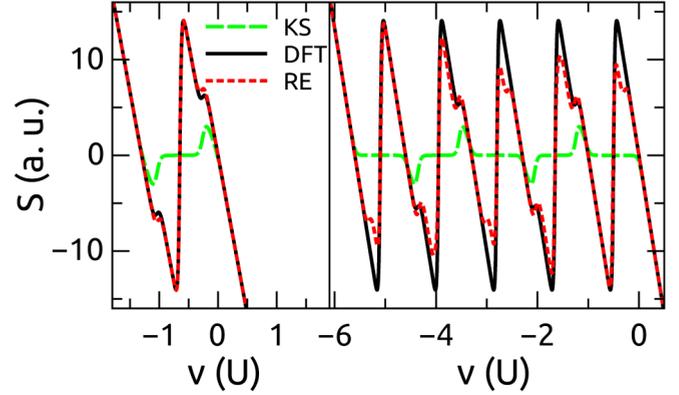
FIG. 3. Seeebeck coefficient for the Anderson model with non-degenerate single-particle levels (left) and for three spin-degenerate levels (right). The parameters are $\varepsilon_\uparrow^0 = 0$, $\varepsilon_\downarrow^0 = 0.3$ (left panel) and $\varepsilon_1^0 = 0$, $\varepsilon_2^0 = 0.3$, $\varepsilon_3^0 = 0.6$ (right panel). In both panels $T = 0.03$ and $\gamma = 0.001$ (all energies in units of U).

states of different N. Accordingly, the DFT Seebeck coefficient is expected to exhibit only those wiggles associated with the addition of one electron in the lowest available level. This is confirmed by the right panel of Fig. 2, where the wiggles associated to the addition energies of excited states are captured by the RE (red) but missed by DFT (black). For improving the agreement between DFT and RE one should abandon the zeroth-order uniform approximation and consider a level-dependent Hxc potential which correctly reproduces the level occupations. To further support this analysis on the relation between the nonuniformity of v_{Hxc} and physical excitations we show in Fig. 3 the Seebeck coefficient for the Anderson model with broken spin degeneracy (left) and for a three-level CIM (right). In the first case DFT agrees with RE since there exists only one addition energy, whereas in the second case DFT misses the wiggles of excited-state addition energies. We emphasize that the wiggles stem from S_s (green line) and are not due to the xc correction. The latter is responsible for the large sawtooth oscillations and, as Figs. 2 and 3 clearly show, it is the dominant contribution to S.

Recently experimental measurements of the Seebeck coefficient and the electrical conductance in the CB regime have been reported for an individual single-wall carbon nanotube [35] as well as for quantum dots [31,32]. For the transport properties of nanotubes, we can extract both single-particle energies and charging energies from the experimental results and then use them to calculate G and S within our DFT scheme. We again consider the Hxc potential of Eq. (8) but, in contrast to the model calculations described previously, the charging energies U_K depend on the charging state K.

In Fig. 4 we plot the conductance G calculated using the formalism of Ref. [8] (upper panel) and the Seebeck coefficient S calculated from Eq. (7) (lower panel) versus the gate voltage v for the parameters of Table I and for temperature $T = 4.5$ K and coupling $\gamma = 0.02$ meV. For comparison we also report the Seebeck coefficient as calculated from the LB-DFT formalism with the same parameters. LB-DFT fails in reproducing the characteristic sawtooth behaviour of the experimental results. Instead, the Seebeck coefficient
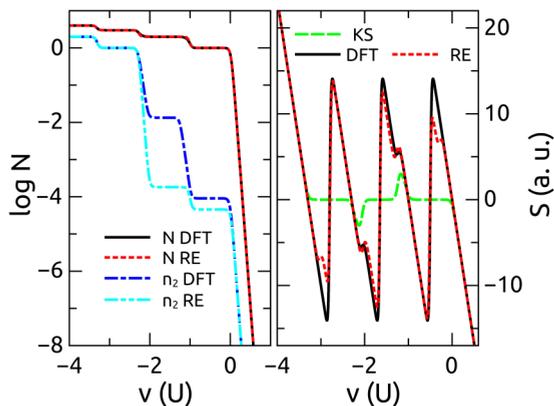

FIG. 2. Density (left) and Seebeck coefficient (right) of CIM with two spin-degenerate levels computed from RE and DFT using the approximate functional of Eq. (8). The KS Seebeck coefficient is also shown.
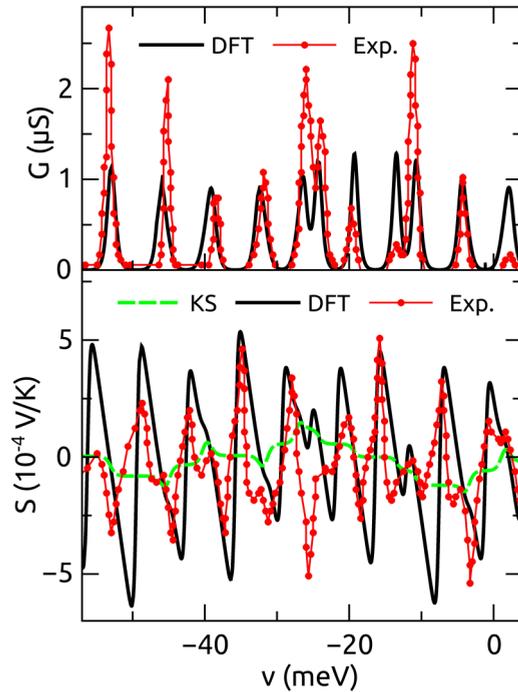
FIG. 4. Conductance (upper panel) and Seebeck coefficient (lower panel) of a single-wall carbon nanotube from DFT (black) and experiment (red, data from Ref. [35]). Also shown is the KS Seebeck coefficient (dashed green). The single particle and charging energies are given in Table I. The other parameters are $T = 4.5$ K and $\gamma = 0.02$ meV.

TABLE I. Single-particle energies ε^0 and charging energies U_K (in meV), for modeling the calculation of Fig. 4.

ε^0	−6.0	−3.75	−3.75	−3.75	−1.5	0.75
K, U_K	1, 3.75	2, 5.0	4, 2.25	6, 4.5	8, 4.5	10.5.25
		3, 6.25	5,5.75	7,2.0	9,6.5	11,6.75

the Coulomb blockade regime. We found that two ingredients in the Hxc potential are essential: (i) the step feature at integer electron number opens a gap in the linear dependence on gate voltage and (ii) the temperature derivative generates the sawtooth behavior in this gap region. Remarkably, the xc correction represents the dominant contribution to S just as the xc correction to the conductance dominates in the Coulomb blockade regime [8]. We have compared our theory with both rate equations and experimental results on a carbon nanotube and found good quantitative agreement in all cases. The present approach is valid in the linear response regime, where the applied thermal gradient is small. Going beyond the linear response would pave the way for a deeper understanding of the thermoelectric effect and allow to study materials for extreme applications. The recently proposed DFT framework for thermal transport by Eich *et al.* [16] appears to be a promising starting point for this purpose.

calculated with our DFT scheme clearly shows the peak and valley structures observed in experiment, confirming again the crucial role of the xc correction. Also, all the fine structure wiggles (kinks in some cases) are correctly captured.

In conclusion, we have proposed a DFT scheme for the calculation of the Seebeck coefficient which corrects the deficiencies of the canonical Landauer-Büttiker approach in

[1] F. J. DiSalvo, Science **285**, 703 (1999).

[2] C. B. Vining, Nat. Mater. **7**, 765 (2008).

[3] C. B. Vining, Nat. Mater. **8**, 83 (2009).

[4] Y. Dubi and M. Di Ventra, Rev. Mod. Phys. **83**, 131 (2011).

[5] H. J. Goldsmid, *Introduction to Thermoelectricity in Springer Ser. Mater. Sci.* (Springer-Verlag, Berlin, 2010).

[6] M. Di Ventra, *Electrical Transport in Nanoscale Systems* (Cambridge University Press, New York, 2008).

[7] R. D'Agosta, Phys. Chem. Chem. Phys. **15**, 1758 (2013).

[8] S. Kurth and G. Stefanucci, Phys. Rev. Lett. **111**, 030601 (2013).

[9] Z.-F. Liu and K. Burke, Phys. Rev. B **91**, 245158 (2015).

[10] G. Stefanucci and S. Kurth, Nano Lett. **15**, 8020 (2015).

[11] G. Stefanucci and C.-O. Almbladh, Phys. Rev. B **69**, 195318 (2004).

[12] G. Stefanucci and C.-O. Almbladh, Europhys. Lett. **67**, 14 (2004).

[13] N. Sai, M. Zwolak, G. Vignale, and M. Di Ventra, Phys. Rev. Lett. **94**, 186810 (2005).

[14] M. Koentopp, K. Burke, and F. Evers, Phys. Rev. B **73**, 121403 (2006).

[15] G. Vignale and M. Di Ventra, Phys. Rev. B **79**, 014201 (2009).

[16] F. G. Eich, M. Di Ventra, and G. Vignale, Phys. Rev. Lett. **112**, 196401 (2014).

[17] F. G. Eich, A. Principi, M. Di Ventra, and G. Vignale, Phys. Rev. B **90**, 115116 (2014).

[18] T. A. Costi and V. Zlatić, Phys. Rev. B **81**, 235127 (2010).

[19] C. W. J. Beenakker, Phys. Rev. B **44**, 1646 (1991).

[20] C. W. J. Beenakker and A. A. M. Staring, Phys. Rev. B **46**, 9667 (1992).

[21] X. Zianni, Phys. Rev. B **78**, 165327 (2008).

[22] J. Cai and G. D. Mahan, Phys. Rev. B **74**, 075201 (2006).

[23] Y. Apertet, H. Ouerdane, C. Goupil, and P. Lecoeur, Eur. Phys. J. Plus **131**, 76 (2016).

[24] B. Dong and X. Lei, J. Phys.: Condens. Matter **14**, 11747 (2002).

[25] H. Haug and A.-P. Jauho, *Quantum Kinetics in Transport and Optics of Semiconductors* (Springer, New York, 2008).

[26] G. Stefanucci and S. Kurth, Phys. Rev. Lett. **107**, 216401 (2011).

[27] E. Perfetto and G. Stefanucci, Phys. Rev. B **86**, 081409 (2012).

[28] P. Tröster, P. Schmitteckert, and F. Evers, Phys. Rev. B **85**, 115409 (2012).

[29] J. P. Bergfield, Z.-F. Liu, K. Burke, and C. A. Stafford, Phys. Rev. Lett. **108**, 066801 (2012).

[30] A. A. M. Staring, L. W. Molenkamp, B. W. Alphenaar, H. van Houten, O. J. A. Buyk, M. A. A. Mabesoone, C. W. J. Beenakker, and C. T. Foxon, Europhys. Lett. **22**, 57 (1993).

[31] A. S. Dzurak, C. G. Smith, M. Pepper, D. A. Ritchie, J. E. F. Frost, G. A. C. Jones, and D. G. Hasko, Solid State Commun. **87**, 1145 (1993).

[32] A. S. Dzurak, C. G. Smith, C. H. W. Barnes, M. Pepper, L. Martín-Moreno, C. T. Liang, D. A. Ritchie, and G. A. C. Jones, Phys. Rev. B **55**, R10197 (1997).

[33] U. Gupta and A. K. Rajagopal, Phys. Rep. **87**, 259 (1982).

[34] G. Stefanucci and S. Kurth, Phys. Status Solidi B **250**, 2378 (2013).

[35] J. P. Small, K. M. Perez, and P. Kim, Phys. Rev. Lett. **91**, 256801 (2003).